Proceedings of the Canadian Society for Mechanical Engineering International Congress 2022
CSME Congress 2022
June 5-8, 2022, Edmonton, AB, Canada

Electromechanical Properties of 3D-Printed Smart Materials for Structural Health Monitoring

Menna A. Saleh[1], Roger Kempers[1], Garrett W. Melenka[1]
[1]Department of Mechanical Engineering, Lassonde School of Engineering, York University, Toronto, Ontario, Canada

Abstract—Smart materials with sensing capabilities are an exciting new technology that will impact many applications, including structural health monitoring (SHM), biomedical implants, wearable sensors, automotive, and actuators. Strain sensors (piezoresistive material) for SHM can be used to measure the in-situ deformation by integrating the structural and sensing function into one component. Conductive polymer composites are being developed for SHM due to their flexibility, low cost, and low processing temperature. However, these materials are usually not durable and are difficult to repair. This study leverages additive manufacturing (AM) to fabricate continuous wire polymer composites (CWPCs) which are self-sensing, multi-functional composite structures wherein a sensor is an integral part of the structure and can enhance its mechanical properties. For this study, electromechanical properties of copper (Cu) reinforced polylactic acid (PLA), nickel-chromium (NiCr) reinforced PLA, and Cu reinforced thermoplastic polyurethane (TPU) were investigated to compare the sensing capabilities of composites using two different types of wires. This manufacturing approach provides sensors with significant design flexibility, repeatability, and lower fabrication time and cost, which helps to widen the range of applications. To achieve these goals, samples of CWPCs have been fabricated and electromechanically characterized successfully in tension and fatigue scenarios to study the correlation between elastic mechanical deformation and electrical resistance.

Keywords-Additive manufacturing; Electromechanical properties; Structural health monitoring; Polymer composites

I. INTRODUCTION

Continuous fiber polymer composites (CFPCs) provide improved specific stiffness, specific strength, thermal and electrical conductivity over short fiber reinforced polymer composites [1-3]. CFPCs have been used in numerous applications such as aerospace, automotive, and sporting equipment industries [1,2], however CFPCs still contend with many problems such as long processing cycle times which leads to high production costs [2]. Common CFPC manufacturing methods include manual hand-layup, vacuum forming, pultrusion, filament winding, compression molding, and bladder assisted molding [4]. Drawbacks of these manufacturing methods include high mold cost, the inability of producing a specific fiber orientation, and the difficulties to manufacture complex construction parts [4]. Additive manufacturing (AM) is becoming increasingly utilized to overcome drawbacks of conventional CFPC production [1,2].

AM is a layer-by-layer manufacturing process which directly converts 3D digital geometries into physical structure [1]. A main advantage of AM over subtractive techniques is the ability to fabricate more complex products. Different techniques with different printing mechanisms are used such as fused filament fabrication (FFF), stereolithography, selective laser sintering, and laminated object manufacturing [5].

Presently, only FFF and stereolithography have been used for (CFPC) fabrication where the continuous fibers can be introduced in-situ and impregnated into the polymer during the process [1,6]. And among these two technologies, FFF (where a continuous fiber is fused along with the thermoplastic material filament through a heated nozzle) is more promising for several reasons. First, it is less demanding technologically as it could be used with modifications to commercially available filament extruders [1]. The modification is mainly conducted to the hot end to be able to introduce both matrix filament and continuous fiber simultaneously [2]. Second, the feedstock materials used in FFF technique have longer shelf life [1]. Third, it is a commercially accessible technology due to its flexibility with low-cost hardware and its large open-source community supporting its continuous development [2]. CFPC components with enhanced mechanical properties can be readily fabricated by AM techniques as reported by several researchers [2,5–8].

Smart materials of conductive polymer composites have gained increasing interest recently due to their improved mechanical properties, flexibility, low cost, and low processing temperature [9,10]. Internal damage in polymer composites is usually difficult to predict compared to isotropic metals, and they require continuous monitoring for any sign of internal damage or failure for safety issues and to increase their lifespan [10].

The system for continuous monitoring of the composite damage is referred to as structural health monitoring (SHM) [11,12]. Among various measurable signals, the one most commonly used is mechanical strain due to its ease of

implementation. Additionally, mechanical strain provides full representation of the health status by delivering physical information including locations of the damage within the structures. Piezoresistive methods in which the mechanical deformation of the structure is correlated to a change in electrical resistance is the most commonly applied method. In this method, the electrical resistance (R) of the structure under mechanical loading is measured and then the strain (ε) is calculated based on the gauge factor (GF) property of the material as in (1) [9,13–15].

$$GF = (\Delta R/R)/\varepsilon. \quad (1)$$

In the field of SHM, most of the available commercial sensors are made from metallic films which have low stretchability and flexibility, and thus limited range of applications. Semiconductor materials were introduced as SHM sensors due to their high piezoresistive sensitivity, yet they have poor mechanical properties [16]. In this respect, conductive polymer composites are highly recommended in the field of SHM where the material can be used to measure the in-situ part deformation.

Most research has focused on laminated continuous carbon fiber polymer composites (CCFPC). Carbon fiber has been chosen as the conductive material to predict the induced strain due to its superior Young's modulus along with high thermal and electrical conductivity; however, if the change of the resistance of CCFPC is small, measurement difficulties arise due to the high stiffness of CCFPC [13,15]. Alternative approaches employed glass fiber reinforced laminated epoxy composites with embedded nickel alloy wire for electrical measurements [13]. However, the use of embedded sensors within the composite structures may cause difficulties like property degradation or delamination which will eventually lead to serious structural damage [15]. The optimum solution to address these shortcomings is through using multi-functional composite structures in which the sensor is an integral part of the structure while simultaneously serving to enhance mechanical properties. This can be achieved by AM of continuous wire polymer composites (CWPCs).

Most AM CFPC or CWPCs research has focused on improving and quantifying the mechanical properties of the AM components. However, there exists the opportunity to explore the piezoresistive capabilities of these types of AM composite—particularly for the electrically conductive metal wires present in CWPCs. Currently, SHM sensors of AM CWPCs has not been examined in particular, integrated AM of strain sensors has not been undertaken.

In this study, CWPCs of copper (Cu) reinforced polylactic acid (PLA), nickel-chromium (NiCr) reinforced PLA, and Cu reinforced thermoplastic polyurethane (TPU) were 3D-printed and their eletromechanical properties were investigated and compared under static (tensile) and dynamic (fatigue) loading conditions. The GF was used to evaluate the performance of 3D-printed CWPCs to be used as piezoresistive strain sensor for structural health monitoring. The mechanical properties in terms of ultimate tensile strength (UTS) and Young's modulus were also studied. Analytical models were presented to compare both mechanical and electrical properties to their corresponding experimental data.

II. Experimental work

A. Sample Preparation

Modification of a low-cost, open-source printer (Prusa i3 mk2, Prusa Research, Prague, Czech Republic) was done as reported by Ibrahim el al. [2] to allow fabrication of CWPCs using the FFF technique. Different matrices such as rigid PLA (1.75 mm Transparent PLA, ColorFabb, The Netherlands) and flexible TPU (1.75 mm Transparent TPU, Ninjatek, USA) and different wire reinforcement materials such as polyimide-coated Cu (75 μm Cu wire, Remington Industries, USA) and uncoated NiCr (75 μm NiCr wire, Consoloidated Electronics Wire & Cable, Illinois, USA) were used to prepare five configurations of the samples: pure PLA, pure TPU, PLA+Cu, PLA+NiCr, and TPU+Cu. Samples were 3D-printed with dimensions of 200 mm x 25 mm x 2 mm according to ASTM D3039 – 17 standard using a customized Matlab script (MATLAB R2019b, Natick, Massachusetts: The MathWorks Inc.). For the Cu CWPC sample, the two wires were extended from one corner at the bottom layer and one corner at the top layer of the printed sample for the electrical resistance to be measured through a single circuit running through all five layers. However, the NiCr CWPC samples used un-coated wires which were susceptible to potential short circuiting between the wires in adjacent layers, particularly in the gripping region at the ends of the sample. To avoid this, the lead wires were extended from only the middle layer circuit and the electrical resistance was measured only in this layer. Fig. 1 shows an example of the 3D-printed sample with wire connections for electrical resistance measurements. Table 1 summarize the printing parameters used to fabricate the samples.

B. Electromechanical Characterization

The electrical resistance of CWPCs samples was recorded in-situ using digital multimeter (DMM) (Agilent 34401A, Agilent Technologies Inc., Colorado, USA) using the 4-wire method. To calculate the GF (1), the extension of the sample during the test was accurately measured using 2D digital image correlation (DIC) system and the strain was then calculated using the DIC software package (DaVis version 10.0.3 StrainMaster, LaVision GmbH, Gottingen, Germany).

For the static tensile tests, the sample was loaded with cross head speed of 2 mm/min using universal test frame (Instron ElectroPlus Model E3000, Norwood, USA). Five samples for each CWPC configuration were tested.

For the dynamic test, sinusoidal wave of strain-controlled fatigue test was conducted using a universal test frame (Series 809 Axial/Torsional Test System, MTS Systems Co., USA) with a maximum strain applied on the sample equivalent to 50% of the maximum strain at failure obtained from the tensile test. To avoid sample compression, strain ratio of R = 0.1 was chosen. Tension-tension cycles was applied at frequency of 5 Hz to avoid material's self-heating. Three samples for each CWPC configuration were tested.

Figure 1. a) Example of 3D-printed CWPC sample with wire connection, b) Enlarged schematic of the sample cross-section.

Table 1. 3D-pronting parameters of CWPCs samples.

	Material Type	
	PLA based material	TPU based materials
Extruder temperature (°C)	200	220
Bed temperature (°C)	50	55
Nozzle diameter (mm)	1	
Raster width (mm)	0.65	
Layer height (mm)	0.4	
Printing angle (°)	0	
Number of rasters	38	
Number of layers	5	
Fill density (%)	100	

C. *Analytical Model*

Since the 3D-printed CWPCs have different mechanical properties in terms of stiffness and tensile strength, it was recommended to use different mechanical analytical models to predict their behavior. For PLA based materials, the rule of mixture (ROM) model was applied since it assumes rigid material with continuous reinforcement. While, for the flexible TPU based material, a hyperelastic analytical model, specifically the Mooney-Rivlin two parameter model was applied to predict the mechanical behavior of the part [17,18].

1) Rule of mixture model: To apply this model, the individual mechanical properties of each constituent should be identified. Table 2 summarizes the properties of Cu and NiCr wires, while, the properties of PLA and TPU were determined from the mechanical tensile testing as mentioned above.

Table 2. Cu and NiCr wires mechanical properties [2].

	Young's modulus	UTS
Cu wire	110 (GPa)	210 (MPa)
NiCr wire	200 (GPa)	689 (MPa)

Equation (2) represents the predicted UTS and Young's modulus of CWPCs [2,17]. The volume fraction of each constituent was determined based on the geometry of the sample and printing parameters such as number of rasters and layers to get the volume fraction of the wires.

$$\sigma_c = V_w\sigma_w + V_p\sigma_p, \tag{2-a}$$

$$E_c = E_wE_w + E_pE_p. \tag{2-b}$$

where σ_c, σ_w, σ_p, E_c, E_w, and E_p are the UTS and Young's modulus of the composite, wire, and polymer, respectively. V_w and V_p are the volume fractions for both wire and polymer, respectively.

For 3D-printed structures, voids are commonly exist within the part due to the nature of the printing process. Accordingly, the ROM model was modified as mentioned by several researchers [17-19].

2) Moneey-Rivlin two parameters model: For this model, the sample should be incompressible under uniaxial load and have a transversely isotropic nature to fulfill (3) and (4) [20].

$$\lambda_1 \lambda_2 \lambda_3 = 1. \tag{3}$$

$$\lambda_1 = \lambda, \tag{4-a}$$

$$\lambda_2 = \lambda_3 = 1/(\lambda^{0.5}). \tag{4-b}$$

where λ is the stretch ratio along the principal axes (λ = 1 + strain).

Equation (5) represents Money-Rivlin analytical model [19]. To get the material parameters in this equation, curve fitting was applied for the experimental stress-stretch curve using Comsol software (Comsol Multiphysics 5.5, Stockholm, Sweden). Afterwards, the stress-strain curve for the analytical model was developed using the obtained material parameters values. This theoretical stress-strain curve was then used to calculate the UTS and Young's modulus of the material to be compared with the experimental results.

$$\sigma_{Mooney} = 2\,(\lambda^2 - (1/\lambda))\,(C_1 + C_2(1/\lambda)). \tag{5}$$

where σ_{Mooney} is applied stresses in a uniaxial direction, and C_1 and C_2, are material parameters.

3) Gauge factor analytical model: The GF analytical model is based on the electrical resistance equation as shown in (6) [21]. Here, the instantaneous change in electrical resistance due to the change of wire geometry (L_i and A_i) under tensile loading was calculated and compared to the initial value of the electrical resistance to calculate the fractional change in electrical resistance (ΔR/R) as shown in (7). Afterwards, GF equation as in (1) was applied to get the relation between the calculated fractional change of electrical resistance and corresponding applied strain on the sample.

$$R_i = (\rho L_i)/A_i. \quad (6)$$

where ρ is the resistivity of the wire material, and L_i, A_i, and R_i are instantaneous values of the wire length, area, and electrical resistance, respectively, corresponding to the instantaneous applied extension.

$$\text{Fractional change of electrical resistance} = (R_i - R)/R. \quad (7)$$

where R_i is the measured resistance of the sample during loading and R is the initial resistance of sample before loading.

Paired sample t-test was applied to check the statistical significance between the analytical and experimental GF data using a confidence level of 95% ($p < 0.05$).

III. Results and Discussion

The UTS and Young's modulus of all 3D-printed configurations are presented in Fig. 2. It can be seen that both composite materials (PLA and TPU based materials) showed improvement in the mechanical properties compared to the corresponding pure materials (PLA and TPU). For PLA based materials, PLA+NiCr has UTS and Young's modulus higher than that of PLA+Cu and this may be attributed to the higher mechanical properties of NiCr wire compared to Cu wire as shown in Table 2. Fig. 2 also shows the comparison between the experimental and analytical model data. Statistical analysis of paired sample t-test with confidence level of 95 % ($p < 0.05$) showed insignificance between these data as shown in Table 3.

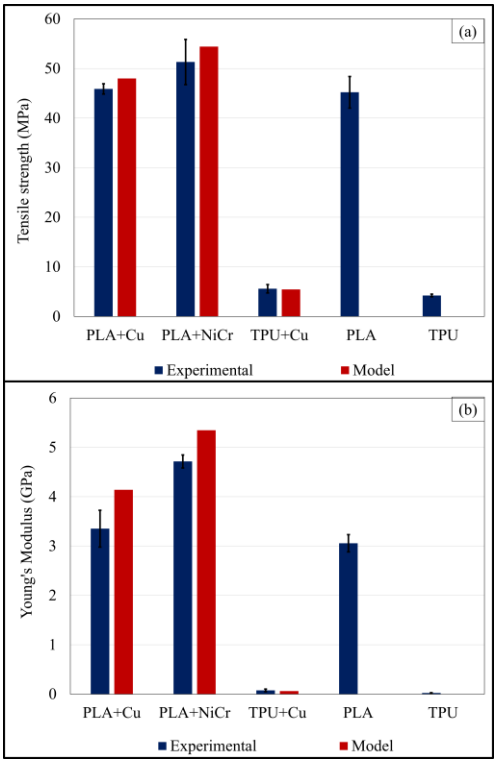

Figure 2. Mechanical properties of 3D-printed materials; a) UTS, b) Young's modulus.

Table 3. Paired sample t-test of analytical model and experimental mechanical properties of 3D-printed parts (NS: statistically not significant).

		P-value	Significance
UTS (Model vs. Exp)	PLA+Cu	0.054	NS
	PLA+NiCr	0.062	NS
	TPU+Cu	0.052	NS
Young's Modulus (Model vs. Exp)	PLA+Cu	0.527	NS
	PLA+NiCr	0.051	NS
	TPU+Cu	0.09	NS

The electromechanical property of CWPCs under tensile test is shown in Fig. 3. In this figure, a direct linear relationship between the fractional change of electrical resistance and the strain is demonstrated, indicating the applicability of these CWPCs materials to be used as a strain sensor. Not only can CWPCs be used to measure strain, but they can also indicate the type of fracture. For instance, PLA+Cu and TPU+Cu showed a sudden increase in the electrical resistance of the Cu wire indicating the breakage of the wire and therefore the failure of the part. While, for PLA+NiCr, the electrical resistance of NiCr wire was gradually increased till the failure of the matrix.

Fig. 4 shows the results of the calculated GF (1) of CWPCs. Also, a comparison between the experimental and analytical model values of the GF is demonstrated in Fig. 4. It can be seen that there is no statistical difference between experimental and analytical model data of GF for all CWPCs with p-value of 0.772, 0.064, and 0.342 for PLA+Cu, PLA+NiCr, and TPU+Cu, respectively.

The uncoated NiCr wire showed some difficulties in measuring its resistance such as fluctuations of the readings for some sample and this may be attributed to a short circuit that could occur between the conductive metal frame of the testing machine and the uninsulated NiCr wire. Therefore, the coated wire is recommended to be used for further studies on this type of CWPCs materials.

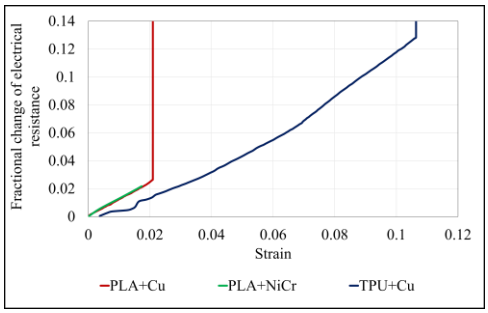

Figure 3. Plot of (ΔR/R-ε) curve of CWPCs.

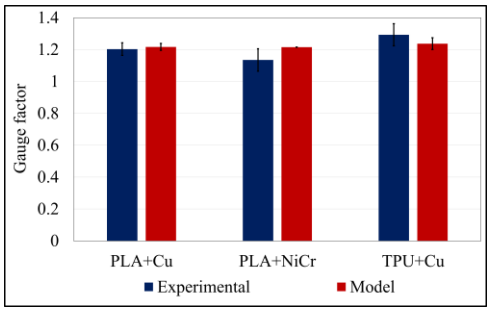

Figure 4. Experimental and analytical model GFs of CWPCs.

Both PLA+Cu and TPU+Cu were tested under fatigue test. The reversible change of strain (primary axis) and the reversible change of electrical resistance (secondary axis) of CWPCs with increasing number of loaded and unloaded cycles are shown in Fig. 5. For PLA+Cu (Fig. 5-a), the wire was broken after approximately 36000 cycles after which the electrical resistance increased suddenly. While, for TPU+Cu (Fig. 5-b), the wire was broken at around 180 cycles. The higher number of cycles for PLA+Cu may be attributed to the maximum applied stress on the sample corresponding to 50% of the failure strain.

The maximum corresponding applied stress was around 67% and 80% of the UTS of PLA+Cu and TPU+Cu, respectively. A small specific range of cycles from 20th cycle to 50th cycle is shown in Fig. 6 to elaborate the reversible change of electrical resistance and strain with the number of cycles for both PLA+Cu (Fig. 6-a) and TPU+Cu (Fig. 6-b). This reverse piezoresistivity behavior of CWPCs indicates the applicability of this type of 3D-printed materials to be used as strain sensor under cyclic loading.

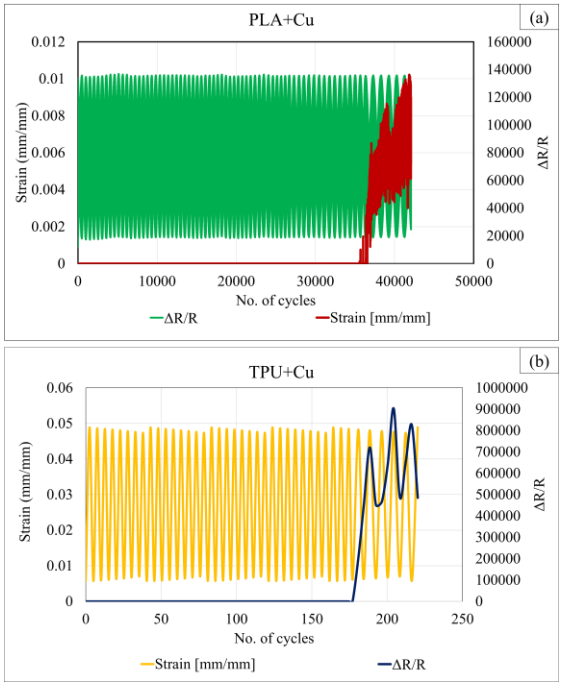

Figure 5. Strain and electrical resistance response of CWPCs under fatigue test; a) PLA+Cu, b) TPU+Cu.

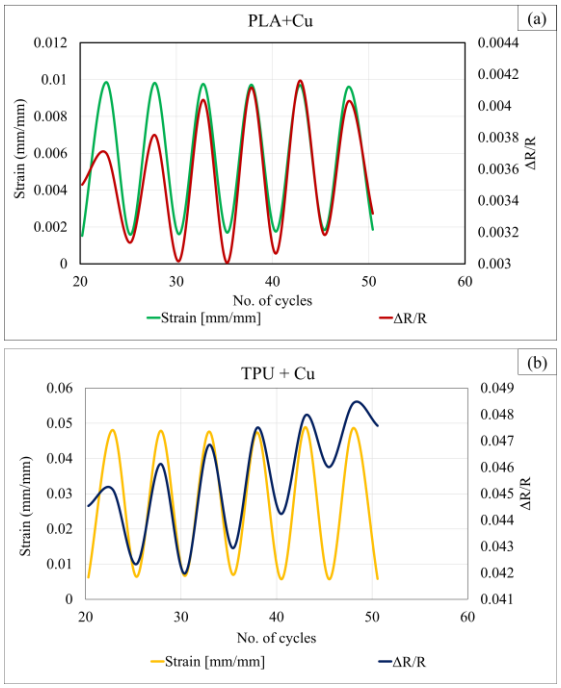

Figure 6. Change in strain and electrical resistance from 20th to 50th cycles; a) PLA+Cu, b) TPU+Cu.

IV. CONCLUSION

Presently, an increase in ultimate tensile strength (UTS) and Young's modulus have been achieved, for PLA and TPU CWPCs printed parts, in addition to including integrated sensing capability due to the linear relationship between the fractional change of electrical resistance and the strain. This verifies the capability of 3D-printing to fabricate sensors with tunable properties.

The electromechanical properties of both composites showed dependency of the strain sensor on the integrated wire, regardless of the type of matrix used.

Both mechanical and electrical analytical models showed statistical agreement with experimental data.

Under cyclic loading, the electrical resistance changed reversibly upon loading and unloading, indicating reverse piezoresistivity behavior of the material for both PLA CWPC and TPU CPWC.

The proposed process will produce low-cost smart materials of AM CWPCs that can be used as strain sensor with improved mechanical properties.

ACKNOWLEDGMENT

The authors would like to thank the Natural Science and Research Council (NSERC) Canada [RGPIN- 2018-05899] for the funding support of this study.

REFERENCES

[1] G. D. Goh, D. Vishwesh, P. N. Arun, L. G. Guo, A. Shweta, L. S. Swee, W. Jun, and Y. Y. Wai, "Characterization of mechanical properties and

fracture mode of additively manufactured carbon fiber and glass fiber reinforced thermoplastics," *Mater. Des.*, vol. 137, pp. 79–89, 2018.

[2] Y. Ibrahim, G. W. Melenka, and R. Kempers, "Fabrication and tensile testing of 3D printed continuous wire polymer composites," *Rapid Prototyp. J.*, vol. 24, no. 7, pp. 1131–1141, 2018.

[3] Y. Ibrahim and R. Kempers, "Efective thermal conductivity of 3D-printed continuous wire polymer composites," *Prog. Addit. Manuf.*, 2022.

[4] C. Yang, X. Tian, T. Liu, Y. Cao, and D. Li, "3D printing for continuous fiber reinforced thermoplastic composites: Mechanism and performance," *Rapid Prototyp. J.*, vol. 23, no. 1, pp. 209–215, 2017.

[5] A. C. De Leon, Q. Chen, N. B. Palaganas, J. O. Palaganas, J. Manapat, and R. C. Advincula, "High performance polymer nanocomposites for additive manufacturing applications," *React. Funct. Polym.*, vol. 103, pp. 141–155, 2016.

[6] A. Gupta and A. A. Ogale, "Dual curing of carbon fiber reinforced photoresins for rapid prototyping," *Polym. Compos.*, vol. 23, no. 6, pp. 1162–1170, 2002.

[7] T. Hofstätter, D. B. Pedersen, G. Tosello, and H. N. Hansen, "State-of-the-art of fiber-reinforced polymers in additive manufacturing technologies," *J. Reinf. Plast. Compos.*, vol. 36, no. 15, pp. 1061–1073, 2017.

[8] R. Matsuzaki, M. Ueda, M. Namiki, T. K. Jeong, H. Asahara, K. Horiguchi, T. Nakamura, A. Todoroki, and Y. Hirano, "Three-dimensional printing of continuous-fiber composites by in-nozzle impregnation," *Sci. Rep.*, vol. 6, pp. 1–7, 2016.

[9] A. Zribi, M. Barthès, S. Bégot, F. Lanzetta, J. Y. Rauch, and V. Moutarlier, "Design, fabrication and characterization of thin film resistances for heat flux sensing application," *Sensors Actuators, A Phys.*, vol. 245, pp. 26–39, 2016.

[10] Y. Elsayed, A. Elkholy, G. Melenka, and R. Kempers, "Continuous Fiber Polymer Composites for Thermal Applications," pp. 1–6, 2018.

[11] R. Balaji and M. Sasikumar, "Graphene based strain and damage prediction system for polymer composites," *Compos. Part A Appl. Sci. Manuf.*, vol. 103, pp. 48–59, 2017.

[12] J. B. Park, T. Okabe, N. Takeda, and W. A. Curtin, "Electromechanical modeling of unidirectional CFRP composites under tensile loading condition," *Compos. - Part A Appl. Sci. Manuf.*, vol. 33, no. 2, pp. 267–275, 2002.

[13] R. Balaji and M. Sasikumar, "Development of strain and damage monitoring system for polymer composites with embedded nickel alloys," *Meas. J. Int. Meas. Confed.*, vol. 111, no. August, pp. 307–315, 2017.

[14] R. Balaji and M. Sasikumar, "A nanometallic nickel-coated, glass-fibre-based structural health monitoring system for polymer composites," *Smart Mater. Struct.*, vol. 26, no. 9, 2017.

[15] G. Y. Lee, M. S. Kim, H. S. Yoon, J. Yang, J. B. Ihn, and S. H. Ahn, "Direct Printing of Strain Sensors via Nanoparticle Printer for the Applications to Composite Structural Health Monitoring," *Procedia CIRP*, vol. 66, pp. 238–242, 2017.

[16] G.W. Melenka, B.K.O. Cheung, J.S. Schofield, M.R. Dawson, J.P. Carey, "Evaluation and prediction of the tensile properties of continuous fiber-reinforced 3D printed structures", *Compos. Struct.*, 153 (2016) 866–875.

[17] M.A. Saleh, R. Kempers, G.W. Melenka, "3D printed continuous wire polymer composites strain sensors for structural health monitoring," *Smart Mater. Struct.*, 28 (2019) 105041.

[18] M.A. Saleh, R. Kempers, G.W. Melenka, "A comparative study on the electromechanical properties of 3D-Printed rigid and flexible continuous wire polymer composites for structural health monitoring." Sensors and Actuators A: Physical 328 (2021): 112764.

[19] J.F. Rodriguezjames, P.T.E. Renaud, J.F. Rodriguez, J.P. Thomas, J.E. Renaud, Characterization of the mesostructure of fused-deposition acrylonitrile-butadiene-styrene materials. Rapid Prototyp. J. (2000).

[20] A. Chanda, S. Chatterjee, V. Gupta, "Soft composite based hyperelastic model for anisotropic tissue characterization," *J. Compos. Mater.*, 54 (2020) 4525–4534.

[21] Ogi K, Takao Y. "Characterization of piezoresistance behavior in a CFRP unidirectional laminate," *Compos Sci Technol.*, 2005;65(2):231–9.